

RESISTIVITY STUDIES ON MN SITE SUBSTITUTED $\text{La}_{0.67}\text{Ca}_{0.33}(\text{Mn}_{1-x}\text{Ga}_x)\text{O}_3$ MANGANITES

BHARAT R. KATARIA¹, CHIRAG SAVALIYA² & J. H. MARKNA³

¹Department of Physics, Government Science College, Jhalod, Gujarat, India

²Department of Nanotechnology, V. V. P. Engineering College, Rajkot, Gujarat, India

³Department of Physics, Saurashtra University, Rajkot, Gujarat, India

ABSTRACT

Effect of Mn-site disorder in $\text{La}_{0.67}\text{Ca}_{0.33}\text{Mn}_{1-x}\text{Ga}_x\text{O}_3$ (LCMGO) created by the substitution of Ga^{3+} at Mn-site is studied through X-ray diffraction (XRD) and temperature dependent resistivity measurements to identify the role of size mismatch at Mn-site and their resistivity property correlations. XRD patterns collected at room temperature for all the LCMGO samples reveal single phasic nature without any detectable impurities within the measurement range studied. XRD data shows that all the samples possess orthorhombic structure without any structural phase transition. Variation in resistivity with Ga^{3+} content has been discussed in detail in the context of modifications in the structural and magnetic lattices and structural disorder.

KEYWORDS: Resistivity Studies on Mn Site Substituted $\text{La}_{0.67}\text{Ca}_{0.33}(\text{Mn}_{1-x}\text{Ga}_x)\text{O}_3$ (LCMGO)

INTRODUCTION

Last two decades have witnessed a phenomenal growth in research on ABO_3 type perovskite structured mixed valent manganites exhibiting colossal magneto resistance (CMR) effect, due to their scientific and technological applications [1 – 3]. Existence of structural disorder in the manganites does not meet the criteria of Zener double exchange (ZDE) mechanism successfully and ZDE cannot alone explain all the physical (transport) properties of CMR manganites. Important role played by the structural strain in revising the transport and magnetic properties of manganites have been investigated [4, 5].

Optimally divalent doped LaMnO_3 are known to exhibit metal to insulator transition at T_p and ferromagnetic to paramagnetic transition at T_C in concomitant with a sharp rise in magnetoresistance (MR) effect around (T_p / T_C) as a origin of intrinsic property / mechanism of CMR. Optimally doped LaCaMnO_3 manganite is well studied in the form of polycrystalline and nanostructured bulk, thin film, nanostructured thin film and device [6 – 11] due to its high magnetic ordering temperature near room temperature (RT) and large magnetoresistance (MR) exhibited around its T_p [6]. In the view point of applications, Jo et al have reported the spin and charge modulated trilayered magnetic tunnel junctions: $\text{La}_{0.7}\text{Ca}_{0.3}\text{MnO}_3 / \text{La}_{0.45}\text{Ca}_{0.55}\text{MnO}_3 / \text{La}_{0.7}\text{Ca}_{0.3}\text{MnO}_3$ and observed a strong magneto-electric coupling [11].

In the view point of fundamental mechanisms and understanding of physics of manganites, several reports are available on the studies on the effect of Mn-site substitution on the transport and magnetic properties of manganites [12 – 19]. It has been well established that, one can control the transport and magnetic properties Mn-site substituted manganites by doping of magnetic as well as non-magnetic ions. Sridharan et al have studied the effect of Zr, Fe and Hf substitution at Mn-site in $\text{La}_{0.67}\text{Ca}_{0.33}\text{MnO}_3$ manganites [12]. Detailed studies on the effect of magnetic ions substitution at Mn^{3+} site on the

ferromagnetic state of $\text{La}_{0.7}\text{Pb}_{0.3}\text{Mn}_{0.8}\text{Me}_{0.2}\text{O}_3$ ($\text{Me} = \text{Ni}^{3+}$, Co^{3+} and Fe^{3+}) manganites [16] wherein the transport and magnetic properties variations have been discussed in the light of magnetic interactions between the Mn^{3+} , Mn^{4+} and Me^{3+} magnetic ions. Studies on substitution of Ti^{4+} doped at Mn-site in $\text{La}_{0.7}\text{Ca}_{0.3}\text{MnO}_3$ manganites show the modifications in the magnetic and transport properties with Ti^{4+} -content [17]. Recently, Tiwari et al have reported the dependence of transport and magnetic properties on the Al^{3+} -content in $\text{La}_{0.7}\text{Ca}_{0.3}\text{Mn}_{1-x}\text{Al}_x\text{O}_3$ [20]. Teresa et al have shown strong magnetic interactions depend on the nonmagnetic Ga^{3+} -content at Mn^{3+} -site in $\text{La}_{2/3}\text{Ca}_{1/3}\text{Mn}_{1-x}\text{Ga}_x\text{O}_3$ manganites [21].

Keeping in mind the above mentioned aspects of Mn-site substitutional effects in manganites, in this chapter the results of the studies on nonmagnetic Ga^{3+} and doped at Mn^{3+} -site in $\text{La}_{0.67}\text{Ca}_{0.33}\text{Mn}_{1-x}\text{Ga}_x\text{O}_3$ system, have been discussed in the context of nonmagnetic phase fraction in the magnetic lattice of Mn ions.

EXPERIMENTAL

Polycrystalline samples of $\text{La}_{0.67}\text{Ca}_{0.33}\text{Mn}_{1-x}\text{Ga}_x\text{O}_3$ (LCMGO) with $x = 0.00, 0.02, 0.04, 0.06, 0.08$ and 0.10 (hereafter referred as G0, G2, G4, G6, G8 and G10, respectively) were synthesized using conventional solid state reaction (SSR) route. La_2O_3 , CaCO_3 , MnO_2 and Ga_2O_3 chemicals purchased from sigma Aldrich with 99.9% purity. The dried starting powders of La_2O_3 , CaCO_3 , MnO_2 and Ga_2O_3 were mixed in stoichiometric proportions and calcined at 950°C for 24 hrs. Samples were then pressed into pellets and sintered at 1050°C for 48 hrs followed by final sintering at 1150°C for 72 hrs. X-ray diffraction (XRD) patterns were noted on Philips diffractometer (PW 3040/60, X'pert PRO) using $\text{CuK}\alpha$ radiation at RT. Structural analysis was carried out using FULLPRUF. For microstructural investigations, scanning electron microscopy (SEM) measurements were carried out at RT and electrical resistivity (temperature range: 5 – 300K) were performed using the standard four probe dc method.

RESULTS AND DISCUSSIONS

In order to understand the structure, structural phases present and phase purity of LCMGO system, XRD studies on all the Ga-doped $\text{La}_{0.67}\text{Ca}_{0.33}\text{Mn}_{1-x}\text{Ga}_x\text{O}_3$ (LCMGO) ($x = 0.00, 0.02, 0.04, 0.06, 0.08$ and 0.10) samples were carried out at room temperature (RT). Figure 1(a) depicts the XRD raw data of all the LCMGO samples showing single phasic nature without any detectable impurities and any structural phase transition. Figure 1(b) shows an enlarged view of most intense (121) XRD peak of LCMGO system depicting the shifting of (121) peak towards higher 2θ degree which can be attributed to the substitution of smaller Ga^{3+} (0.62\AA) at larger Mn^{3+} (0.645\AA) site and hence enhancement in lattice parameters and unit cell volume.

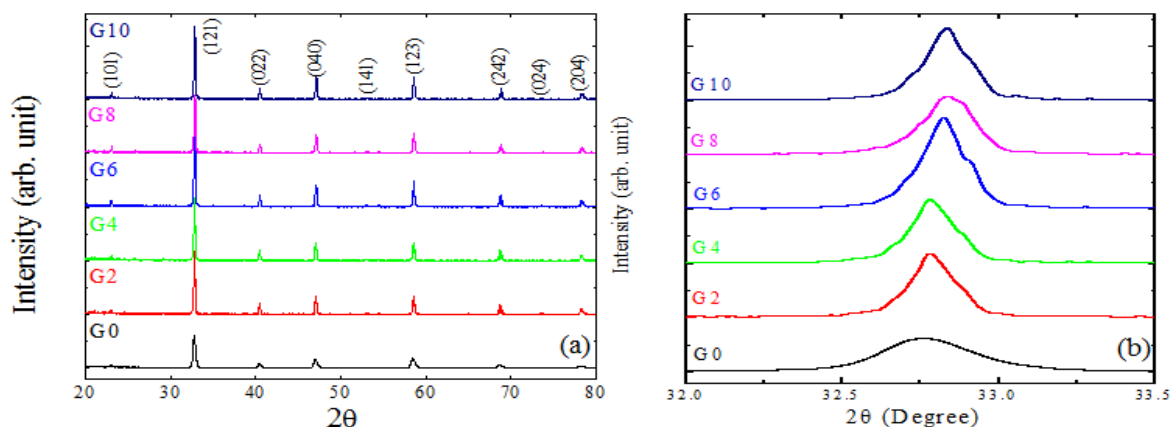


Figure 1: (a) XRD Patterns of LCMGO Samples (b) Enlarge View of (121) XRD Peak of LCMGO Samples

Microstructure SEM Studies

SEM micrographs, obtained out at RT, for all the LCMGO samples, are shown in figure 2. It can be seen that, all the samples studied possess island and flat disc like granular structures with an average grain size in the micrometer range.

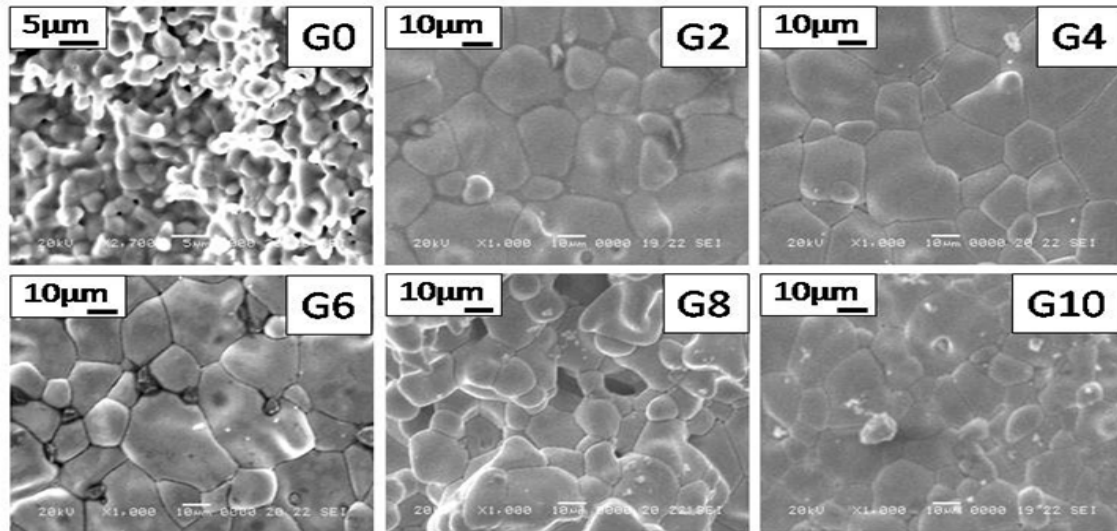


Figure 2: SEM Micrographs of LCMGO Samples

Four Probe Resistivity Measurements

Variation in resistivity (in logarithmic scale) with temperature (range: 5 – 300K) under zero applied field is shown in figure 3(a) for all the LCMGO samples studied.

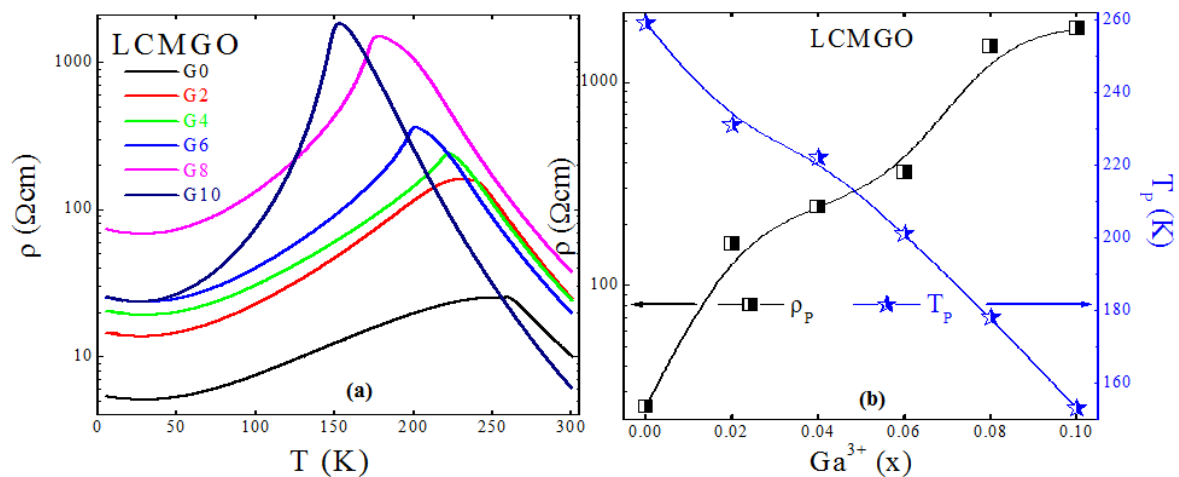


Figure 3: (a) Temperature Dependence of Resistivity (in Logarithmic Scale) under Zero Applied Field for LCMGO Samples (b) Variation in T_P and ρ_P (in Logarithmic Scale) with Ga^{3+} - Content (x) for LCMGO Samples

It can be seen that, all the LCMGO samples studied show the metal ($d\rho / dT > 0$) to insulator ($d\rho / dT < 0$) transition at temperature T_P . At T_P , all the samples show a peak resistivity, ρ_P , below (above) which the resistivity decreases with decreasing (increasing) temperature. The values of T_P and ρ_P are tabulated in Table 1. It can be seen that, with increase in Ga^{3+} - content (x), from G0 to G10, the resistivity increases monotonically while T_P shifts towards lower temperature. Figure 3(b) shows the variation in T_P and ρ_P (in logarithmic scale) with x for LCMGO samples.

Table 1: Values of Resistivity at Peak (ρ_p) and Transition Temperature (T_p) for $\text{La}_{0.67}\text{Ca}_{0.33}\text{Mn}_{1-x}\text{Ga}_x\text{O}_3$ Samples

Sample Code & Content (x)	Peak Resistivity (ρ_p) (Ωcm)	Transition Temperature T_p (K)
G0 (0.00)	25.42	259
G2 (0.02)	159.81	231
G4 (0.04)	243.51	222
G6 (0.06)	361.84	201
G8 (0.08)	1501.12	178
G10 (0.10)	1843.26	153

CONCLUSIONS

- Studies on structural, transport properties dependence on the smaller ionic sized nonmagnetic Ga^{3+} substitution at the larger ionic sized magnetic Mn^{3+} site have been discussed in this chapter in the light of structural and magnetic disorder effects. FULLPRUF analysis of $\text{La}_{0.67}\text{Ca}_{0.33}\text{Mn}_{1-x}\text{Ga}_x\text{O}_3$ (LCMGO) manganites revealed the single phasic nature of all the samples without any detectable impurity phases present in the samples, having orthorhombic unit cell structure.
- Resistivity studies show the systematic variation in resistivity and metal to insulator transition temperature (T_p) with Ga^{3+} content (x) which is attributed to the ionic size variation and magnetic nature difference induced modifications in the structural and magnetic lattices.
- Low temperature minima observed below 35K in all the samples studied have been understood on the basis of electron – electron scattering mechanism due to weak localization and structural disorder in the manganites. Metallic region of the resistivity vs temperature plots of all the LCMGO samples and studied zener double exchange polynomial law. Magnetic lattice modifications due to nonmagnetic Ga^{3+} substitution at magnetic Mn^{3+} lattice site.

REFERENCES

1. K. Chahara, T. Ohno, M. Kasai and Y. Kosono, Appl. Phys. Lett. 63 (1993) 1990.
2. R. Von Helmolt, J. Wecker, B. Holzapfel, L. Schultz and K. Samwer, Phys. Rev. Lett. 71 (1993) 2331.
3. S. Jin, T.H. Tiefel, M. McCromack, R.A. Fastnacht, R. Ramesh and L.H. Chen, Science 264 (1994) 413.
4. H.Y. Hwang, S.W. Cheong, P.G. Radelli, M. Marezio and B. Batlogg, Phys. Rev. Lett. 75(1995) 914.
5. R.P. Sharma, G.C. Xiong, C. Kwon, R. Ramesh, R.L. Greene and T. Venkatesan, Phys. Rev. B 54 (1996) 10014.
6. R. Mahendiran, R. Mahesh, A.K. Raychaudhuri and C.N.R. Rao, Phys. Rev. B 53, 12160 (1996)
7. P.K. Siwach, U.K. Goutam, Pankaj Srivastava, H.K. Singh, R.S. Tiwari and O.N. Srivastava, J. Phys. D: Appl. Phys. 39, 14 (2006)
8. M. Petit, M. Rajeswari, A. Biswas, R.L. Greene, T. Venkatesan and L.J. Martinez-Miranda, J. Appl. Phys. 97, 093512 (2005)
9. M.A. Lopez-Quintela, L.E. Hueso, J. Rivas and F. Rivadulla, Nanotechnology 14, 212 (2003)
10. M.A. Paranjape, K.S. Shankar and A.K. Raychaudhuri, J. Phys. D: Appl. Phys. 38, 3674 (2005)

11. M.H. Jo, M.G. Blamire, D. Ozkaya and A.K. Petford-Long, J. Phys.: Condens. Matter 15, 5243 (2003)
12. V. Sridharan, L.S. Lakshmi, R. Govindraj, R. Nithya, D.V. Natarajan and T.S. Radhakrishnan, J. Alloys Comp. 326, 65 (2001)
13. Y. Sun, X. Xu, W. Tong and Y. Zhang, Appl. Phys. Lett. 77, 2734 (2000)
14. Y. Sun, W. Tong, X. Xu, Y. Zhang, Appl. Phys. Lett. 78, 643 (2001)
15. L.K. Leung and A.H. Morrish, Phys. Rev. B 15, 2485 (1977)
16. S.L. Young, Y.C. Chen, H.Z. Chen, L. Horng and J.F. Hsueh, J. Appl. Phys. 91, 8915 (2002)
17. X. Liu, X. Xu and Y. Zhang, Phys. Rev. B 62, 15112 (2000)
18. J. Blasco, J. Garcia, J.M. De Teresa, M.R. Ibarra, J. Perez, P.A. Algarabel, C. Marquina and C. Ritter, Phys. Rev. B 55, 8905 (1997)
19. D.N.H. Nam, L.V. Bau, N.V. Khiem, N.V. Dai, L.V. Hong, N.X. Phue, R.S. Newrock and P. Nordblad, Phys. Rev. B 73, 184430 (2006)
20. Shailja Tiwari, D.M. Phase, R.J. Choudhary, H.S. Mund and B.L. Ahuja, J. Appl. Phys. 109, 033911 (2011)
21. J.M. De Teresa, P.A. Algarabel, C. Ritter, J. Blasco, M.R. Ibarra, L. Morellon, J.I. Espeso and J.C. Gomez-Sal, Phys. Rev. Lett. 94, 207205 (2005)

